

The (d , ${}^2\text{He}$) reaction on ${}^{96}\text{Mo}$ and the double- β decay matrix elements for ${}^{96}\text{Zr}$

H. Dohmann,¹ C. Bäumer,^{1,*} D. Frekers,¹ E.-W. Grewe,¹ M. N. Harakeh,² S. Hollstein,¹ H. Johansson,^{3,†} L. Popescu,^{4,‡} S. Rakers,^{1,§} D. Savran,^{2,5} H. Simon,³ J. H. Thies,¹ A. M. van den Berg,² H. J. Wörtche,² and A. Zilges⁶

¹*Institut für Kernphysik, Westfälische Wilhelms-Universität, D-48149 Münster, Germany*

²*Kernfysisch Versneller Instituut, University of Groningen, NL-9747 AA Groningen, The Netherlands*

³*Gesellschaft für Schwerionenforschung, D-63291 Darmstadt, Germany*

⁴*Vakgroep Subatomaire en Stralingsfysica, Universiteit Gent, B-9000 Gent, Belgium*

⁵*Institut für Kernphysik, Technische Universität Darmstadt, D-64289 Darmstadt, Germany*

⁶*Institut für Kernphysik, Universität zu Köln, D-50937 Köln, Germany*

(Received 9 April 2008; published 15 October 2008)

The ${}^{96}\text{Mo}(d, {}^2\text{He}){}^{96}\text{Nb}$ charge-exchange reaction was investigated at an incident energy of $E_d = 183.5$ MeV. An excitation-energy resolution of 110 keV was achieved. The experiment was performed at KVI, Groningen, using the magnetic spectrometer BBS at three angular positions: 0° , 2.5° , and 6° . We found that below 6 MeV almost the entire Gamow-Teller (GT^+) strength is concentrated in a single state at 0.69 MeV excitation energy. As ${}^{96}\text{Mo}$ is the daughter of the $\beta\beta$ decay nucleus ${}^{96}\text{Zr}$, the present result provides information about the nuclear matrix elements active in the $2\nu\beta\beta$ decay of ${}^{96}\text{Zr}$.

DOI: [10.1103/PhysRevC.78.041602](https://doi.org/10.1103/PhysRevC.78.041602)

PACS number(s): 25.45.Kk, 25.55.-e, 23.40.Hc, 27.60.+j

I. Introduction. Intermediate energy (d , ${}^2\text{He}$) charge-exchange reactions have become an established tool to study Gamow-Teller (GT) transitions in the β^+ direction [1–12]. Together with the intermediate energy (${}^3\text{He}$, t) reactions, which are now being routinely performed with the highest resolution at the Research Center for Nuclear Physics (RCNP), Osaka [5, 13, 14], these two types of charge-exchange reactions can rather effectively be used for a precise experimental determination of $2\nu\beta\beta$ -decay matrix elements [2, 3, 5–7]. The typical resolution of the (n , p)-type (d , ${}^2\text{He}$) reaction is of the order of 100 keV, which, together with the 30 keV resolution for the (p , n)-type (${}^3\text{He}$, t) reaction, constitutes more than an order of magnitude improvement over past experiments using the elementary (n , p) or (p , n) reactions performed at the TRIUMF CHARGEX setup or the IUCF SWINGER facility [15–18]. This high resolution is, in fact, an important requirement for getting deeper insight into the physics of GT transition, as was shown in recent studies performed in the context of $\beta\beta$ decay [2, 5–7]. Information about GT^+ and GT^- strength distribution can give significant guidance to theoretical models that are aimed at calculating $\beta\beta$ -decay matrix elements, in this case foremost those involving the 2ν decay and to a lesser extent those involving the neutrinoless ($0\nu\beta\beta$) decay [19, 20]. These matrix elements are needed for the rates estimates of many of the large-scale experiments that are presently operational or soon will be [21–28].

The present charge-exchange experiment addresses the nuclear matrix elements of the ${}^{96}\text{Zr}$ $\beta\beta$ decay from the (n , p)-type direction, i.e., starting from the $\beta\beta$ -decay daughter ${}^{96}\text{Mo}$. Recently, NEMO-3 [25–27] measured the $2\nu\beta\beta$ -decay half-life of ${}^{96}\text{Zr}$ to be $T_{1/2} = [2.2 \pm 0.4(\text{stat})] \cdot 10^{19}$ yr [29], which is close to the mean of the half-life values from geochemical methods of $T_{1/2} = [3.9 \pm 0.9] \cdot 10^{19}$ yr and $T_{1/2} = [0.94 \pm 0.32] \cdot 10^{19}$ yr [30, 31]. One may note that the ${}^{96}\text{Zr}$ 2ν half-life is of the same size as those of many $\beta\beta$ emitters in the mass $A \sim 100$ region, like ${}^{82}\text{Se}$, ${}^{100}\text{Mo}$, ${}^{116}\text{Cd}$, and ${}^{150}\text{Nd}$ [26, 29, 32–41]. On the other hand, theoretical estimates for the alternative 0ν -decay variant show that ${}^{96}\text{Zr}$ represents a rather singular case, as nuclear structure models based on the QRPA predict rather unfavorable matrix elements for this decay [19, 42]. Of course, the 0ν decay follows a path that is quite different from that of the $2\nu\beta\beta$ decay. We will show that the nuclear structure of ${}^{96}\text{Zr}$ also exhibits some remarkable features pertaining to the $2\nu\beta\beta$ -decay mode.

A sketch of the 2ν path is shown in Fig. 1 showing that the GT^- (p , n)-type and the GT^+ (n , p)-type transitions are, in usual jargon, the two “legs”, which provide the information about, the matrix element that is active for the decay. As the present experiment only addresses GT^+ (n , p)-type transitions, the final evaluation of the $2\nu\beta\beta$ -matrix element will have to await further information about the GT^- leg, which necessitates an experiment of (p , n) type, like, e.g., ${}^{96}\text{Zr}({}^3\text{He}, t){}^{96}\text{Nb}$, which, as was shown in Refs. [5] and [6], can successfully be performed at the RCNP facility in Osaka.

II. Experiment. The (d , ${}^2\text{He}$) charge-exchange experiment was performed at the AGOR cyclotron facility of the KVI, Groningen [43–45], using a deuteron beam at an incident energy of $E_d = 183.5$ MeV. Outgoing protons were momentum analyzed in coincidence by the BBS-ESN-setup [44, 45]. The ESN-detector consists of a focal-plane detection system with two vertical drift chambers and a second detector with four multiwire proportional chambers [46, 47]. The momenta of the two outgoing protons from the (d , ${}^2\text{He}$) reaction are usually

*Present address: Philips Research Europe, Weisshausstr. 2, 52066 Aachen, Germany.

†Present address: Fundamental Fysik, Chalmers Tekniska Högskola, S-412 96, Göteborg, Sweden.

‡Present address: KVI, University of Groningen, NL-9747 AA Groningen.

§Present address: EADS Astrium Space Transportation GmbH, TE53 Avionics Engineering, 28199 Bremen, Germany.

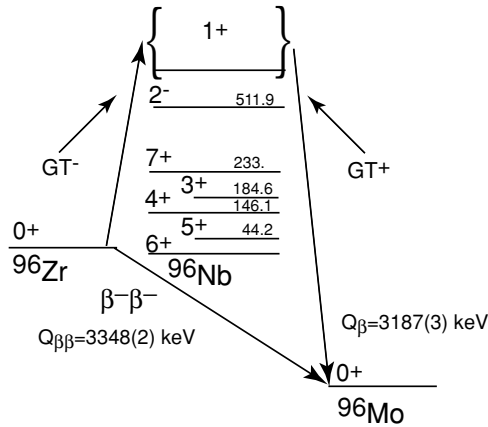


FIG. 1. Schematic representation of the $2\nu\beta^-\beta^-$ decay of ^{96}Zr and the low-energy level scheme of the intermediate nucleus ^{96}Nb . The intermediate states in the 2ν decay mode are 1^+ states only. GT^+ refers to (n, p) -type reactions and GT^- to (p, n) -type reactions. The single β^- decay to ^{96}Nb is energetically possible but suppressed by angular momentum. Excitation energies are given in keV.

of the same magnitude as the ones from the deuteron breakup, whose cross section is larger by several orders of magnitude and approximately scales with Z^2 . Although the breakup rate is enormous, the coincident detection of the two protons from the $(d, ^2\text{He})$ reaction ensures largely background-free spectra and the final offline analysis further reduces random correlations. The details of the detection techniques and the offline analyses are given in Ref. [43].

The target consisted of a self-supporting metallic Mo foil enriched to 96.76% of ^{96}Mo with a thickness of 2.67 mg/cm². The $(d, ^2\text{He})$ reaction Q value on ^{96}Mo is $Q = -4.629$ MeV, ensuring that the $(d, ^2\text{He})$ reaction on hydrogen—the latter being an ever-present contamination in metals—is well separated from the ground-state transition of the $^{96}\text{Zr}(d, ^2\text{He})^{96}\text{Nb}$ reaction and appears at 0° at ~ -2.4 MeV in the excitation-energy frame of ^{96}Nb . Spectra were taken at spectrometer angles of 0°, 2.5°, and 6°. The data sets were divided into two and three angle bins depending on statistics. Beam currents were measured by a Faraday cup and ranged from 0.4 to 1.8 nA. The total detection efficiency including the tracking efficiency of the analysis software was evaluated to be 85%.

The energy calibration of the spectra was performed using the reaction from the hydrogen contamination and its kinematic shift as a function of the spectrometer setting. Figure 2 shows the measured excitation-energy spectrum of the $^{96}\text{Mo}(d, ^2\text{He})^{96}\text{Nb}$ reaction at $\Theta_{\text{BBS}} = 0^\circ$ and $\Theta_{\text{BBS}} = 2.5^\circ$ with an energy resolution 110 keV. The background level below zero excitation energy gives an indication of the general remaining instrumental background over the spectrum, whose shape is independent of the excitation energies considered here.

III. Data analysis. The zero-degree spectrum given in Fig. 2 shows a remarkable feature. Only one strong transition near 0.69 MeV is observed together with an indication of a possible weak transition at its low energy tail and another cluster of weak transitions near 2.2 MeV, which becomes

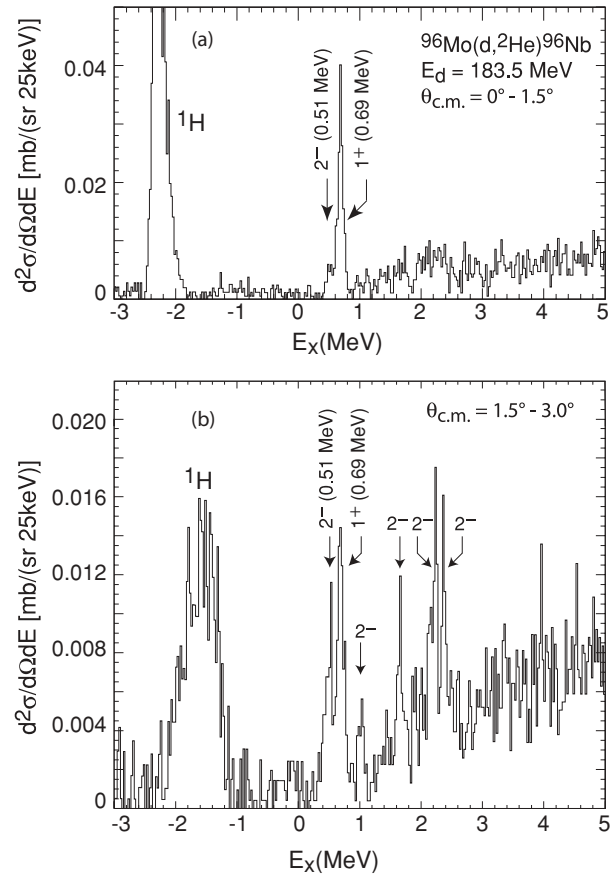


FIG. 2. Excitation-energy spectra for $^{96}\text{Mo}(d, ^2\text{He})^{96}\text{Nb}$. The upper spectrum covers an angular range of $0^\circ \leq \Theta_{\text{c.m.}} \leq 1.5^\circ$ and the lower one a range of $1.5^\circ \leq \Theta_{\text{c.m.}} \leq 3.0^\circ$. The peaks near excitation energy of -2.3 MeV (top panel) and around -1.6 MeV (bottom panel) are due to the ^1H contamination and their width is due to kinematic broadening. The energy resolution is 110 keV.

visible only at larger scattering angles. No further transitions above the general reaction background are observed up to an excitation energy of 15 MeV, neither in the spectra at zero degree nor in those at larger angles. (Note that the background above 1 MeV is a result of the high level density in the odd-odd nucleus ^{96}Nb and not of instrumental nature.) The two components of the peak at 0.69 MeV clearly reveal themselves when following the spectra to larger angles with one state appearing at 0.51 MeV and the other at 0.69 MeV. The two states exhibit different shapes of the angular distribution, of which the one at 0.69 MeV is uniquely determined as a $J^\pi = 1^+$, GT transition and the one at 0.51 MeV as a $J^\pi = 2^-$ transition. The transitions at higher excitation energies near 2.2 MeV exhibit a $J^\pi = 2^-$ character.

Cross sections for the $(d, ^2\text{He})$ reaction are defined as the ε -integrated cross sections covering a relative pp energy range $0 \leq \varepsilon \leq 1$ MeV. For further details about how to extract these cross sections we refer to Refs. [1] and [43].

At intermediate energies the J^π values of individual transitions can be differentiated by the specific shape of the cross-section angular distributions, of which the GT transitions are unique, as they exhibit a characteristic fall-off with

increasing scattering angle. This property is quite robust and largely independent of the underlying model wave functions. Further, GT transitions are mediated by the $\sigma\tau$ component of the effective interaction, which, at zero momentum transfer $q_{tr} = 0$, is by far the strongest component and thereby gives rise to a high level of selectivity [18,48–50]. This is what is observed in the spectrum in Fig. 2.

DWBA calculations were performed with the ACCBA code of Okamura [51] using the adiabatic approximation. As input we took the deuteron optical-model parameters interpolated from Ref. [52]. The outgoing proton optical-model parameters were taken from Ref. [53] and the t -matrix nucleon-nucleon interaction from Love and Franey [54] for an extrapolated projectile energy of 90 MeV. Transition amplitudes were generated using the code NORMOD [55] with occupation numbers based on the shell model with a smeared Fermi surface.

In Figs. 3(a) and 3(b) experimental angular distributions and DWBA model calculations are shown for the states at $E_x = 0.51$ MeV and for $E_x = 0.69$ MeV indicating a $J^\pi = 2^-$ value for the state at 0.51 MeV and $J^\pi = 1^+$ for the one at 0.69 MeV. As the two states are rather closely spaced making

a clear distinction difficult, we have also taken the approach of analyzing them together. The result of the sum is shown in Fig. 3(c). The angular-distribution analysis of the cluster of states around 2.2 MeV is shown in Fig. 3(d), where we attempted a multipole decomposition with a $\Delta L = 0$ and a $\Delta L = 1$ component, which are the only ones to consider near zero momentum transfer. The angular distribution is reproduced by a $J^\pi = 2^-$ transition with a small $J^\pi = 1^+$ component. The significance of the $J^\pi = 1^+$ component being of GT type is, however, rather weak, given also the fact that at this cross-section level weak tensor contributions may start to play a role [56–59].

$B(\text{GT})$ transition-strength values were extracted from the cross-section angular distributions at zero momentum transfer according to [1–9]

$$\left(\frac{d\sigma(q_{tr}=0)}{d\Omega}\right)_{(d,{}^2\text{He})} = C \left(\frac{\mu}{\pi\hbar^2}\right)^2 \frac{k_f}{k_i} N_D J_{\sigma\tau}^2 B(\text{GT}^+). \quad (1)$$

The distortion factor $N_D = 0.026$ was derived (using the ACCBA code) from the ratio of the distorted-wave (DW) to plane-wave (PW) cross sections:

$$N_D = \frac{\sigma_{\text{DW}}(q_{tr}=0)}{\sigma_{\text{PW}}(q_{tr}=0)}, \quad (2)$$

The scaling factor C was taken from previous ($d, {}^2\text{He}$) studies to be $C = 0.320 \pm 0.027$ [4,6]. This value also gives consistent results for the pf shell nuclei ${}^{48}\text{Ti}$ [2], ${}^{50}\text{V}$ [8], and ${}^{51}\text{V}$ [9]. The isovector spin-flip part of the effective interaction at an incident energy of 90 MeV is $J_{\sigma\tau} = 165 \text{ MeV fm}^3$. The strong state at $E_x = 0.69$ MeV then exhibits a strength of $B(\text{GT}^+) = 0.29 \pm 0.08$. In quoting this value, some caution may be in order. In many previous ($d, {}^2\text{He}$) experiments [1,2,4–6,8,9] the scaling factor C of Eq. (1) could be confirmed independently, either by employing isospin symmetry or known $\log ft$ values or by comparing with previous intermediate energy (n, p) measurements. In the present analysis such an independent cross-check is not possible. The high reaction cross section of the deuteron breakup in the Coulomb field of a high- Z target like ${}^{96}\text{Mo}$ ($Z = 42$) may cause a lowering of this factor, thereby leading to an increased value of the extracted $B(\text{GT}^+)$ strength. On the other hand, in a recent analysis of the ${}^{64}\text{Zn}(d, {}^2\text{He})$ reaction [6] this factor turned out to be a reliable quantity at least up to masses $A \sim 65$ and $Z \simeq 30$; therefore, with some caution in mind one may extrapolate to $Z = 42$.

In the present reaction on ${}^{96}\text{Mo}$ the conversion of any of the two $g_{9/2}$ valence protons into a $g_{7/2}$ neutron can proceed largely unhindered and should, in fact, give rise to several comparatively strong GT transitions. However, as this is not observed, one is led to conclude that, if there is any appreciable GT^+ strength located at higher excitation energies, it must be highly fragmented, with individual components clearly carrying less strength than the present detection limit of about 0.03 units. If this were in fact the case, one would be left with the question as to why fragmentation leaves the state at 0.69 MeV so largely unaffected. The neutron separation threshold lies at 6.9 MeV, therefore a coupling to the neutron-decay channel cannot be responsible

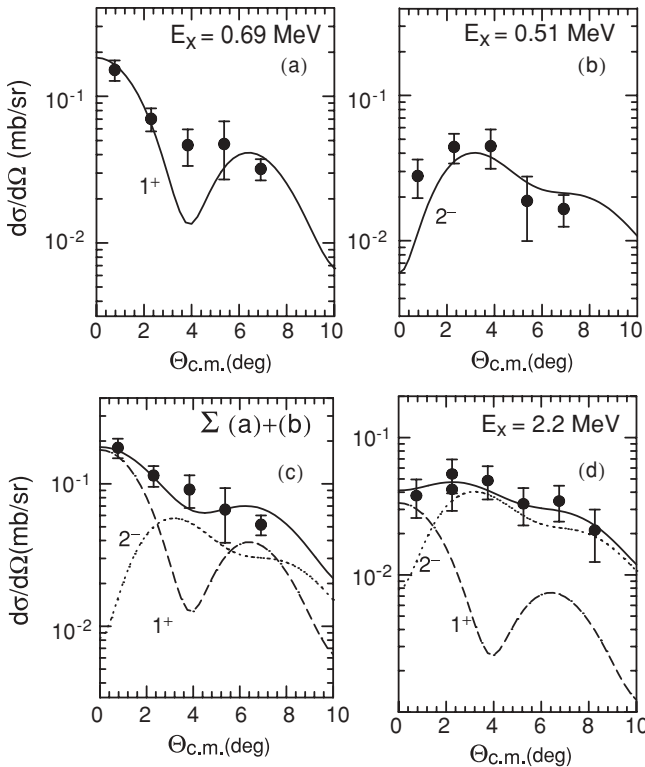


FIG. 3. Angular distributions for the transitions to the levels at 0.69 MeV (a) and 0.51 MeV (b) and the cluster of levels around 2.2 MeV (d) in ${}^{96}\text{Nb}$. The top figures (a) and (b) show the attempt of an individual analysis of the two states in the doublet at 0.51 and 0.69 MeV and the bottom left figure (c) shows a combined analysis. The 2^- strength of the 0.51 MeV transition in part (c) was slightly scaled up compared to the one in the part (b), which could be an indication of another 2^- state appearing at the high-energy tail of the 0.69 MeV 1^+ transition. For the cluster of states around 2.2 MeV a bin size from 2.1 to 2.5 MeV was taken for the combined analysis.

for an enhanced spreading below this energy. An attempt to perform a multipole decomposition of the energy-integrated response does not provide evidence for weak GT transitions either, but we also caution that, without a description of the underlying background, a multipole decomposition remains largely inconclusive.

IV. Occurrence of 2^- states. Whereas the $2\nu\beta\beta$ -decay path almost exclusively proceeds through GT transitions to intermediate 1^+ states in ^{96}Nb , the $0\nu\beta\beta$ path is much more complex as the virtual neutrino may now carry a substantial momentum ($\sim 0.5 \text{ fm}^{-1}$). This allows many intermediate and comparatively high J levels to contribute to the final $0\nu\beta\beta$ -decay matrix element. Of course, the $0\nu\beta\beta$ -decay mode is the more interesting one, as it would reveal the character of the neutrino as being a Majorana particle and, at the same time, it yields its effective mass. Many theoretical models indicate that the intermediate 2^- states could in fact provide the leading contribution to the final $0\nu\beta\beta$ -decay matrix element [60]. It is therefore interesting to note that apart from only one low-lying 1^+ level at 0.69 MeV we observe quite a significant number of low-lying 2^- states at 0.51, 1.02, 1.66, 2.12, 2.24, and 2.37 MeV (cf. Fig. 2), which could well contribute to the matrix elements for the $0\nu\beta\beta$ mode. Unfortunately, because of the different operator active for exciting 2^- states in hadronic reactions, one cannot easily relate the strength observed in the charge-exchange reaction with the one in the weak-interaction process of $\beta\beta$ decay.

V. Corollary. In Fig. 1 the low-energy level scheme of ^{96}Nb is shown. The presently observed state at 0.51 MeV is consistent in energy with the known level at 511.9 keV, and our analysis supports the still tentative spin-parity assignment of

$J^\pi = 2^-$ quoted in the database of the National Nuclear Data Center, Brookhaven [61]. The 0.69 MeV level, on the other hand, matches the known 687.0 keV level, which has been given a tentative $J^\pi = 3^-$ assignment by Cochavi *et al.* [62] in a $^{96}\text{Zr}(p, n\gamma)$ experiment. (Note that this level was slightly corrected to 694.2 keV in Ref. [61].) Because the present charge-exchange reaction is unambiguous as far as the GT transition is concerned, we could suggest that the spin-parity of the 687.0(694.2) keV level should rather be $J^\pi = 1^+$. Through lifetime measurements Cochavi *et al.* [62] also deduced that this state feeds the 2^- state at 511.9 keV via a dipole transition, which would be consistent with either spin assignment. Four out of the five levels above 1 MeV, i.e., at 1.02, 2.12, 2.24, and 2.37 MeV are known as well [61], but have not been given any spin assignment. We suggest for all of them a $J^\pi = 2^-$ assignment.

IV. Conclusion. We have measured the GT^+ strength distribution in the $^{96}\text{Mo}(d, ^2\text{He})^{96}\text{Nb}$ reaction. The total GT strength was found to be mainly concentrated in one level at around 0.69 MeV containing a strength of $B(\text{GT}^+) = 0.29$. This surprising result certainly has an effect on the rate of the $2\nu\beta\beta$ decay. An evaluation of this rate still requires an experiment to measure the GT^- distributions via a (p, n) -type charge-exchange reaction to combine both distributions to a nuclear matrix element for the $2\nu\beta\beta$ decay of ^{96}Zr . Taking the known 2ν -decay rate [32], one can as well predict a $B(\text{GT}^-)$ value needed to arrive at this value, which would be about 0.18 units assuming an unquenched axial-vector coupling constant g_A . A number of low-lying 2^- states were identified, which could be important candidates for intermediate excitations in the $0\nu\beta\beta$ -decay mode.

-
- [1] S. Rakers *et al.*, Phys. Rev. C **65**, 044323 (2002).
 [2] S. Rakers *et al.*, Phys. Rev. C **70**, 054302 (2004).
 [3] S. Rakers *et al.*, Phys. Rev. C **71**, 054313 (2005).
 [4] E.-W. Grewe *et al.*, Phys. Rev. C **69**, 064325 (2004).
 [5] E.-W. Grewe *et al.*, Phys. Rev. C **76**, 054307 (2007).
 [6] E.-W. Grewe *et al.*, Phys. Rev. C **77**, 064303 (2008).
 [7] E.-W. Grewe *et al.*, Phys. Rev. C **78**, 044301 (2008).
 [8] C. Bäumer *et al.*, Phys. Rev. C **71**, 024603 (2005).
 [9] C. Bäumer *et al.*, Phys. Rev. C **68**, 031303(R) (2003).
 [10] C. Bäumer *et al.*, Phys. Rev. C **71**, 044003 (2005).
 [11] L. Popescu *et al.*, Phys. Rev. C **75**, 054312 (2007).
 [12] A. Negret *et al.*, Phys. Rev. Lett. **97**, 062502 (2006).
 [13] T. Adachi *et al.*, Phys. Rev. C **73**, 024311 (2006).
 [14] Y. Fujita *et al.*, Phys. Rev. Lett. **95**, 212501 (2005).
 [15] R. Madey *et al.*, Phys. Rev. C **40**, 540 (1989).
 [16] C. D. Goodman *et al.*, IEEE Trans. Nucl. Sci. **26**, 2248 (1979).
 [17] R. L. Helmer *et al.*, Phys. Rev. C **55**, 2802 (1997).
 [18] R. Helmer, Can. J. Phys. **65**, 588 (1987).
 [19] V. A. Rodin, A. Faessler, F. Šimkovic, and P. Vogel, Phys. Rev. C **68**, 044302 (2003).
 [20] O. Civitarese and J. Suhonen, Nucl. Phys. **A761**, 313 (2005).
 [21] Gerda Collaboration, LNGS P38/04 (2004).
 [22] Majorana Collaboration, arXiv:nucl-ex/0311013 (2003).
 [23] C. E. Aalseth, Phys. At. Nucl. **67**, 2002 (2004).
 [24] H. Nakamura *et al.*, J. Phys. Conf. Ser. **39**, 350 (2006).
 [25] D. Dassie *et al.*, Nucl. Instrum. Methods Phys. Res., Sect. A **309**, 465 (1991).
 [26] R. Arnold *et al.*, Nucl. Instrum. Methods Phys. Res., Sect. A **536**, 79 (2005).
 [27] R. Arnold *et al.*, Nucl. Instrum. Methods Phys. Res., Sect. A **354**, 338 (1995).
 [28] K. Zuber, Phys. Lett. **B519**, 1 (2001).
 [29] R. Arnold *et al.*, Phys. Rev. Lett. **95**, 182302 (2005).
 [30] A. Kawashima, K. Takahashi, and A. Masuda, Phys. Rev. C **47**, R2452 (1993).
 [31] M. E. Wieser and J. R. De Laeter, Phys. Rev. C **64**, 024308 (2001).
 [32] A. S. Barabash, Czech. J. Phys. **56**, 5 (2006).
 [33] D. Dassie *et al.*, Phys. Rev. D **51**, 2090 (1995).
 [34] A. S. Barabash *et al.* Phys. Lett. **B345**, 408 (1995).
 [35] R. Arnold *et al.*, Nucl. Phys. **A636**, 209 (1998).
 [36] F. A. Danevich *et al.*, Phys. Rev. C **62**, 045501 (2000).
 [37] F. A. Danevich *et al.*, Phys. Rev. C **68**, 035501 (2003).
 [38] H. Hidaka, C. V. Ly, and K. Suzuki, Phys. Rev. C **70**, 025501 (2004).
 [39] X. Sarazin, Nucl. Phys. B, Proc. Suppl. **143**, 221c (2005).
 [40] M. J. Hornish, L. De Braeckeleer, A. S. Barabash, and V. I. Umatov, Phys. Rev. C **74**, 044314 (2006).
 [41] R. Saakyan (NEMO3 Collaboration), preliminary values for ^{116}Cd and ^{150}Nd communicated-DBD06-Workshop ILIAS-WG1, Valencia (2006).

- [42] V. Rodin *et al.*, Nucl. Phys. **A766**, 107 (2006).
[43] S. Rakers *et al.*, Nucl. Instrum. Methods Phys. Res., Sect. B **481**, 253 (2002).
[44] A. M. van den Berg, Nucl. Instrum. Methods Phys. Res., Sect. B **99**, 637 (1995).
[45] H. J. Wörtche, Nucl. Phys. **A687**, 321c (2001).
[46] M. Hagemann *et al.*, Nucl. Instrum. Methods Phys. Res., Sect. A **437**, 459 (1999).
[47] V. M. Hannen *et al.*, Nucl. Instrum. Methods Phys. Res., Sect. A **500**, 68 (2003).
[48] C. D. Goodman *et al.*, Phys. Rev. Lett. **44**, 1755 (1980).
[49] T. N. Taddeucci *et al.*, Nucl. Phys. **A469**, 125 (1987).
[50] K. P. Jackson *et al.*, Phys. Lett. B **201**, 25 (1988).
[51] H. Okamura, Phys. Rev. C **60**, 064602 (1999).
[52] A. Korff *et al.*, Phys. Rev. C **70**, 067601 (2004).
[53] A. J. Koning and J. P. Delaroche, Nucl. Phys. **A713**, 231 (2003).
[54] W. G. Love and M. A. Franey, Phys. Rev. C **24**, 1073 (1981).
[55] M. A. Hofstee *et al.*, Nucl. Phys. **A588**, 729 (1995).
[56] R. G. T. Zegers *et al.*, Phys. Rev. C **74**, 024309 (2006).
[57] A. L. Cole *et al.*, Phys. Rev. C **74**, 034333 (2006).
[58] Y. Fujita *et al.*, Phys. Rev. C **75**, 057305 (2007).
[59] R. G. T. Zegers *et al.*, Phys. Rev. C **77**, 024307 (2008).
[60] O. Civitarese and J. Suhonen, Phys. Lett. **B626**, 80 (2005).
[61] National Nuclear Data Center, Brookhaven National Lab, Upton, NY 11973-5000, URL: <http://www.nndc.bnl.gov>, (2007).
[62] S. Cochavi *et al.*, Phys. Rev. C **5**, 164 (1972).